Outdoor performance of the black globe temperature sensor on a hot and humid tropical region

Juan A. Acero [a,b], Angela Dissegna [b], Yon Sun Tan [a], Adrian Tan [c] and Leslie K. Norford [d]

[a] CENSAM, Singapore-MIT Alliance for Research and Technology (SMART), Singapore, Singapore; [b]Singapore-ETH Centre (SEC), Singapore, Singapore; [c] School of Social Sciences, Singapore Management University (SMU), Singapore, Singapore; [d] Department of Architecture, Massachusetts Institute of Technology (MIT), MA, USA

Published in Environmental Technology (2023) 44 (7), 961-973. DOI: 10.1080/09593330.2021.1989057

ABSTRACT: A crucial variable to evaluate thermal comfort is the mean radiant temperature (Tmrt). In this paper we evaluate the performance of the 150 mm black globe thermometer to provide reliable Tmrt values for outdoor settings in Singapore. Accurate Tmrt values are calculated by the method of integral radiation measurements. Based on these, the mean convection coefficient of the black globe has been re-calibrated. Results show an improvement in the estimation of Tmrt with the new coefficient in comparison with the default version suggested in ISO7726:1998. Increasing the averaging periods of the measured variables improved the performance of the derived mean convective coefficients to estimate Tmrt. During clear skies day and for 10-min averaged data, RMSE for Tmrt reduce to 3.9 °C (7.4 °C for ISO7726:1998 coefficient) with an overestimation on high incoming solar radiation periods and an underestimation during the morning and evening (low solar elevation). During overcast dry conditions an underestimation of Tmrt is also expected which is higher in the rain/wet periods. The mean convective coefficient presented in this work can provide improved estimations of Tmrt relevant for outdoor thermal comfort studies in hot and humid tropical climates like Singapore.

Keywords: Black globe thermometer, mean radiant temperature, Singapore, calibration, mean convection coefficient

Calibrated mean convection coefficient
(150 mm black globe)

$$0.82 \cdot 10^{8} \cdot V_a^{0.46}$$

Corresponding author: Juan A. Acero juanangel@smart.mit.edu, CENSAM, Singapore-MIT Alliance for Research and Technology (SMART), 1 Create Way, #09-03, Singapore 138602, Singapore

Nomenclature

T_{mrt}	mean radiant temperature, °C
ISO	International Organization for Standardization
T_g	globe temperature, °C
V_a	wind speed, m s^{-1}
T_a	air temperature, °C
D	globe diameter, m
ε_g	globe emissivity
S_{str}	mean radiant flux reaching a cylindrical representation of the standing human body, Watt m^{-2}
α	albedo of clothed human body
$K_{dir,tot}$	direct and reflected horizontal shortwave radiation in directions E, S, W, N, Watt m^{-2}
K↑	upward shortwave radiation, Watt m^{-2}
K↓	downward shortwave radiation, Watt m^{-2}
K_{diff}	horizontal diffuse radiation in directions E, S, W, N, Watt m^{-2}
ε	emissivity of clothed human body
w_i	surface fractions of the standing cylinder man (coefficients)
L_i	longwave radiation, Watt m^{-2}
Σ	the Stefan Boltzmann constant
T_{mrt_rad}	mean radiant temperature derived from integral radiation measurements, °C
$T_{mrt(Tg)}$	mean radiant temperature derived from globe thermometer data (T_g), °C
$T_{mrt(Tg)\_ISO}$	mean radiant temperature derived from globe thermometer data (T_g) as in ISO7726:1998, °C
$T_{mrt(Tg)\_sing}$	mean radiant temperature derived from a non-linear regression that best fits the measured T_g to the integral radiation measurements(in all weather conditions), °C
$T_{mrt(Tg)\_sing\_nr}$	mean radiant temperature derived from a non-linear regression that best fits the measured T_g to the integral radiation measurements (only in dry conditions), °C
RMSE	root mean square error
$RMSE_s$	systematic root mean square error
$RMSE_u$	unsystematic root mean square error
MAE	mean absolute error
IoA	Index of agreement
r	pearson correlation coefficient

1. Introduction

Air temperature, wind speed, humidity and mean radiant temperature (T_{mrt}) are the four climate variables that influence the human energy balance and thus condition thermal comfort [1] as well as human economic activities [2]. In outdoor environments, mean radiant temperature is the most important parameter under high levels of solar radiation [3–7].

T_{mrt} is defined as the 'uniform temperature of an imaginary enclosure in which radiant heat transfer from the human body is equal to the radiant heat transfer in the actual non-uniform enclosure' [8]. In this sense, T_{mrt} can vary significantly inside urban areas due to the inhomogeneity of radiation fluxes [3,9,10]. Also different conditions of the atmosphere (e.g. cloudiness) affect incoming solar radiation [11–13], and consequently T_{mrt}.

There are different methods to evaluate outdoor T_{mrt} [5]. One approach is direct measurement of shortwave and longwave radiation fluxes (i.e. integral radiation measurements) together with specific angular factors dependent on the incident radiation direction and the body posture [9,12–14]. This approach is a costly and complex measurement technique. Another much simpler method, is the use of a globe thermometer. This was initially developed for the use in indoor environments [15–17]. However, it does not allow to differentiate the effects of short and longwave radiation fluxes on T_{mrt}. Also different coatings of the globe thermometer affect the absorption of radiation [18]. Thorsson et al. [13] showed that a grey globe was suitable to represent the absorption of shortwave radiation by a clothed human body. Some limitations of the globe thermometer related to heat transfer can be overcome through the widely used correction factor for forced air movement proposed by Richard de Dear [15]. However, this factor does not account for highly turbulent conditions occurring outdoors [14], and other factors could be derived for different convection and radiation environments as well as different sizes of globe thermometers. However, the performance and accuracy of the different devices to measure T_{mrt} will vary [19,20]. These studies have reported a systematic underestimation of the mean radiant temperature predicted by small globes that can reach more than 10 °C in forced convection and at high radiative loads.

Finally, several models are able to calculate T_{mrt} with different approximations when dealing with the complexity radiation fluxes in urban environments [10]. Some well-known models for outdoor environment are Rayman [21], ENVI-met [22] and Solweig [23].

The globe thermometer was introduced by Vernon in 1932 as a way to assess the combined effects of radiation, air temperature and air velocity on human comfort. It consists of a 150 mm diameter copper sphere painted black with a thermometer positioned in the middle of the sphere. However, this device could take up to 20 minutes to reach an equilibrium with the local outdoor conditions [24]. Smaller globe sensors than Vernon's have also been used in outdoor spaces, showing that reliable T_{mrt} measurements were reached in shorter periods of time [25]. This could be relevant if the sensor is exposed to frequent changes on radiation fluxes [13].

The theory of the black globe thermometer [16] considers that the temperature measured by the globe thermometer at equilibrium results from a balance between the heat gained and lost by radiation and convection [8]. Knowing air temperature, wind speed and globe

temperature, T_{mrt} can be calculated by:

$$T_{mrt} = \left[(T_g + 273.15)^4 + \frac{1.10 \cdot 10^8 \cdot V_a^{0.6}}{\varepsilon_g \cdot D^{0.4}} (T_g - T_a) \right]^{1/4} - 273.15 \quad (1)$$

where T_g is the globe temperature (°C), V_a is the wind speed (m s^{-1}), T_a is the air temperature (°C), D is the globe diameter (m) and ε_g is the globe emissivity. In our case $\varepsilon_g = 0.95$ (for black globe).

The globe's mean convection coefficient ($1.10 \cdot 10^8 V_a^{0.6}$) has been derived for the case of heat transfer by forced convection between the air and the globe [8], and is typically used for indoor environments. Recently a study in Singapore for an experimental pavilion outdoors (but under negligible solar radiation levels) has shown the necessity of a mixed convection correction to account also for the natural/free convection specially when the gradient between the air and surface temperatures in the space increases and wind speeds are very low (< 0.3 m s^{-1}) [26]. Other studies have evaluated different heat transfer convection coefficients (forced and natural convection) for globe thermometers [20]. However, wind speed in outdoor environment is generally higher than indoors and thus forced convection of heat transfer can be more relevant. In this sense, the mean convection coefficient in Equation (1) could be re-calibrated to adapt the equation to the local outdoor conditions. This approach to improve the estimation of T_{mrt} is commonly used with different size of globe sensors in different latitudes [13,14,27]. In Singapore, a 38 mm globe sensor was calibrated [28].

This study focuses on the analysis of the performance of the standard 150 mm black globe thermometer to provide T_{mrt} values in the hot and humid tropical urban area of Singapore. Specific mean convection coefficients are derived for Equation (1) by comparison with radiant flux measurements (shortwave and longwave). The analysis is carried out in different weather conditions and considers different averaging periods.

2. Methodology

2.1 Study region

Singapore is characterized by a hot and humid climate. The Koppen climate classification is tropical rainforest (Af), characterized by uniform high temperatures along the year (~27.5° C), high relative humidity and significant precipitation ~2190 mm [29].

Regional climate throughout the year is mostly governed by Asian monsoons. They influence cloudiness, surface wind speed, and wind direction [30]. Higher precipitation levels occur in the first two months of the northeast (NE) monsoon season (December to March). However, February and March are much drier and similar to the southwest (SW) monsoon season (June to September), although with different wind pattern. Between these two seasons periods of low winds occur (close to calm situations, especially inland) with variable wind direction. These are the Inter-Monsoon season.

A complete day with clear skies is not common in Singapore. Overcast days are frequent which affect the global incoming solar radiation (both the relation between direct and diffuse components as well as the total amount). Rain precipitation usually occurs only during part of day and can happen in small spatial extend [31,32].

2.2 Site of experiment

Our experiment site is located in the Cantonment Towers, Tanjong Pagar district, Singapore. The site is a modern social housing compound with a playground surrounded by high-density housing blocks. Figure 1. (a) shows the study site with the position of measurement station marked in red and (b) the sensor's set up of the measurement station.

2.3 Sensors and measurement campaigns

The sensors used in this study include three net radiometers Kipp and Zonen CNR4, a Vaisala WXT520 weather station and a Campbell Scientific 150 mm black globe thermometer mounted on a mobile platform to record net radiation, wind speed, precipitation, air temperature, and globe temperature, respectively. The sensors were mounted 1.5 m from the ground. This corresponds to the minimum height suggested by manufacturer to avoid interference with radiometer readings from the mounting structure. Each net radiometer was oriented to a specific direction (North–South, East –West, Up–Down). Special care was made to keep the tower leveled and oriented towards geodetic north.

Radiation measurements obtained for each of the six directions were recorded from 20th February to 2nd March 2020 between 9:30 and 19:00 with a time step of one minute. T_{mrt} was estimated using the integral radiation measurement technique [1,33]. The calculation of the mean radiant flux (S_{str}) reaching a rotationally symmetrical (cylindrical) representation of the standing human body [34] was based on angular factors using Equation (2). Additional information on the characteristics of the approach and the measurement campaign

Figure 1. (a) Location of the measurement station within the study site. (b) Bio-climate measuring station setup, from Dissegna et al. [35].

can be found in Dissegna et al. [35].

$$Sstr = (1\text{-}\alpha)*\left[w_{Cylwall} \cdot \sum_{i=1}^{4} K_{dir,\,tot} + w_{Cylroof} \cdot (K_{\uparrow} + K_{\downarrow}) + 0.22 \cdot \sum_{i=1}^{4} K_{diff} \right] + \varepsilon * \sum_{i=1}^{6} w_i \cdot L_i \quad (2)$$

where

α is the albedo of clothed human body (0.37)

$K_{dir,tot}$ is the direct and reflected horizontal shortwave radiation in directions E, S, W, N

K↑, K↓ is the vertical shortwave radiation (direct + diffuse)

K_{diff} is the horizontal diffuse radiation in directions E, S, W, N

ε is emissivity of clothed human body (0.97)

w_i is Surface fractions of the standing cylinder man ($w_{Cylwall} = 0.28$ and $w_{Cylroof} = 0.0616$)

L_i is Longwave radiation

Then, the T_{mrt} is determined using Equation (3)

$$Tmrt = \sqrt[4]{\frac{S_{str,\,cyl}}{\varepsilon \cdot \sigma}} - 273.15 \quad (3)$$

where

S_{str} is the mean radiant flux

ε is the emissivity of clothed human body

σ is the Stefan Boltzmann constant ($5.670374419 \times 10^{-8}$ $Wm^{-2}K^{-4}$)

2.4 Evaluation of performance of the globe thermometer

Different mean convection coefficients were calculated by systematically comparing the integral radiation measurements (T_{mrt_rad}) with the globe thermometer records (T_g). Three mean convection coefficients were used to translate the globe temperature (T_g) measurements to mean radiant temperature: (a) the empirically derived mean convection coefficient as presented in Equation (1), mostly used for indoor environments, resulting in $T_{mrt(Tg)\_ISO}$; (b) the convection coefficient derived from a non-linear regression that best fits the measured T_g in all weather conditions to the data derived from the integral radiation measurements (T_{mrt_sing}); and (c) the convection coefficient calculated the same way as in (b) but removing the rain/wet periods, i.e. only dry periods ($T_{mrt\,(Tg)\_sing\_nr}$).

In this work we have considered rain/wet periods when the precipitation sensor registered any amount of rain, as well as the following 20 minutes after the precipitation ended. This after-precipitation period was also included in the rain/wet period to allow the evaporation of droplets remaining in the surface of the sensors. This way we tried to assure identification of real dry periods

when higher T_{mrt} values (critical for Singapore) are registered.

Considering the time required for the globe sensor to reach the equilibrium with respect to outdoor conditions, different averaging periods were considered. A specific mean convection coefficient was derived for each averaging period including the whole set of records (rain/wet and dry periods). The performance of the different coefficients were evaluated with several quantitative metrics: The root mean squared error (RMSE) including its derived systematic (RMSEs) and unsystematic (RMSEu) components, the mean average error (MAE), the Pearson correlation coefficient (r) and the dimensionless index of agreement (IoA) defined by Willmott [36].

The performance evaluation of the estimated mean radiant temperature was carried out on one hand for rain/wet periods and on the other for dry periods. Also different mean convection coefficients derived from different averaging periods (1, 3, 5, 10, 15, 20 and 25 minute averages) were analysed.

3. Results and discussion

3.1 Influence of weather conditions

We analyzed the influence of cloudiness and precipitation in the estimation of T_{mrt} determined from 1 min globe temperature (T_g), air temperature (T_a) and wind speed (V_a) measurements.

Three different values of mean radiant temperature (T_{mrt_rad}, $T_{mrt(Tg)\_ISO}$, $T_{mrt(Tg)\_sing}$) have been compared in three days, each with a different weather condition. Results are presented in Figure 2. Two days, 21st and 24th February registered low levels of incoming global radiation due to overcast conditions during most part of the day. Also periods of precipitation occurred. On the contrary, 29th of February was a clear skies day in Singapore.

From the results shown in Figure 2 it is clear that $T_{mrt(Tg)\_ISO}$ and $T_{mrt(Tg)\_sing}$ underestimate T_{mrt_rad} during rain periods and for ~45 minutes after precipitation ends. In low global shortwave radiation (K↓) conditions and well after a precipitation period (e.g. 21st February after 15:30) $T_{mrt(Tg)\_ISO}$ and $T_{mrt(Tg)\_sing}$ show mostly similar values. In cloudy conditions T_g is low and the difference with respect to T_a is lower than in clear skies conditions. Thus, the adaptation of the convection coefficient in Equation (1) will not produce relevant differences in the estimation of mean radiant temperature.

These two estimations show relevant differences with respect to T_{mrt_rad} under short-term radiation changes. As already mentioned in the literature [13,14, 37], $T_{mrt(Tg)\_ISO}$ and $T_{mrt(Tg)\_sing}$ are not capable of capturing quick variations of K↓. Additionally, the results suggest that the underestimation during the rain/wet periods could be influenced by droplets on the surface of the globe thermometer, affecting the radiative balance and producing misleading T_g records.

On the other hand, during clear skies days and high levels of incoming global radiation, $T_{mrt(Tg)\_ISO}$ and $T_{mrt(Tg)\_sing}$ overestimate T_{mrt_rad}. In this case, the influence of the short-wave radiation is overestimated by the globe's albedo since the black colour of the sensor represents a higher albedo than what can be expected in a standing person. On 29th February, sharp reductions of K↓ are not registered in 1-min $T_{mrt(Tg)\_ISO}$ and $T_{mrt(Tg)\_sing}$ values. Under shadow conditions (morning and evening) both $T_{mrt(Tg)\_ISO}$ and $T_{mrt(Tg)\_sing}$ are underestimated influenced by the spherical shape of the globe sensor (further discussion is presented in Section 3.2.2).

Table 1 shows a statistical analysis of the performance of 1-min $T_{mrt(Tg)\_ISO}$ and $T_{mrt(Tg)\_sing}$ values with respect to T_{mrt_rad} for specific periods of each day: (a) dry periods, and (b) rain/wet periods. Aligned with what is shown in Figure 2, RMSE is always higher during the rain/wet periods than in dry periods. On the 21st of February RMSE for $T_{mrt(Tg)\_sing}$ was 7.2 °C and 5.8 °C for rain/wet and dry periods respectively. During the rain/wet periods, the systematic errors ($RMSE_s$) of $T_{mrt(Tg)}$ are high and the unsystematic errors ($RMSE_u$) do not approach the RMSE magnitudes, indicating that there are causes/errors that occur consistently (i.e. systematic underestimation of both $T_{mrt(Tg)\_ISO}$ and $T_{mrt(Tg)\_sing}$). However, this is not the case during the dry periods, when the $RMSE_u$ is higher than $RMSE_s$ showing that differences are inconsistent, i.e. variations in T_{mrt_rad} are not registered by $T_{mrt(Tg)}$ due to low response time of the globe thermometer. Also IoA shows that $T_{mrt(Tg)\_ISO}$ and $T_{mrt(Tg)\_sing}$ perform much better during dry periods.

During the clear skies day (29th February), $RMSE_s$ is much lower for $T_{mrt(Tg)\_sing}$ (4.4 °C) than for $T_{mrt(Tg)\_ISO}$ (8.6 °C) showing that a mean convection coefficient adapted for Singapore, in the case of clear skies, performs much better than the generic one presented in Equation (1).

3.2 Performance of T_{mrt} with different convection coefficients

3.2.1 Influence of averaging periods

Section 3.1 has shown the black globe thermometer is unable to capture short-term variation of K↓ since the sensor needs time to reach a thermal equilibrium

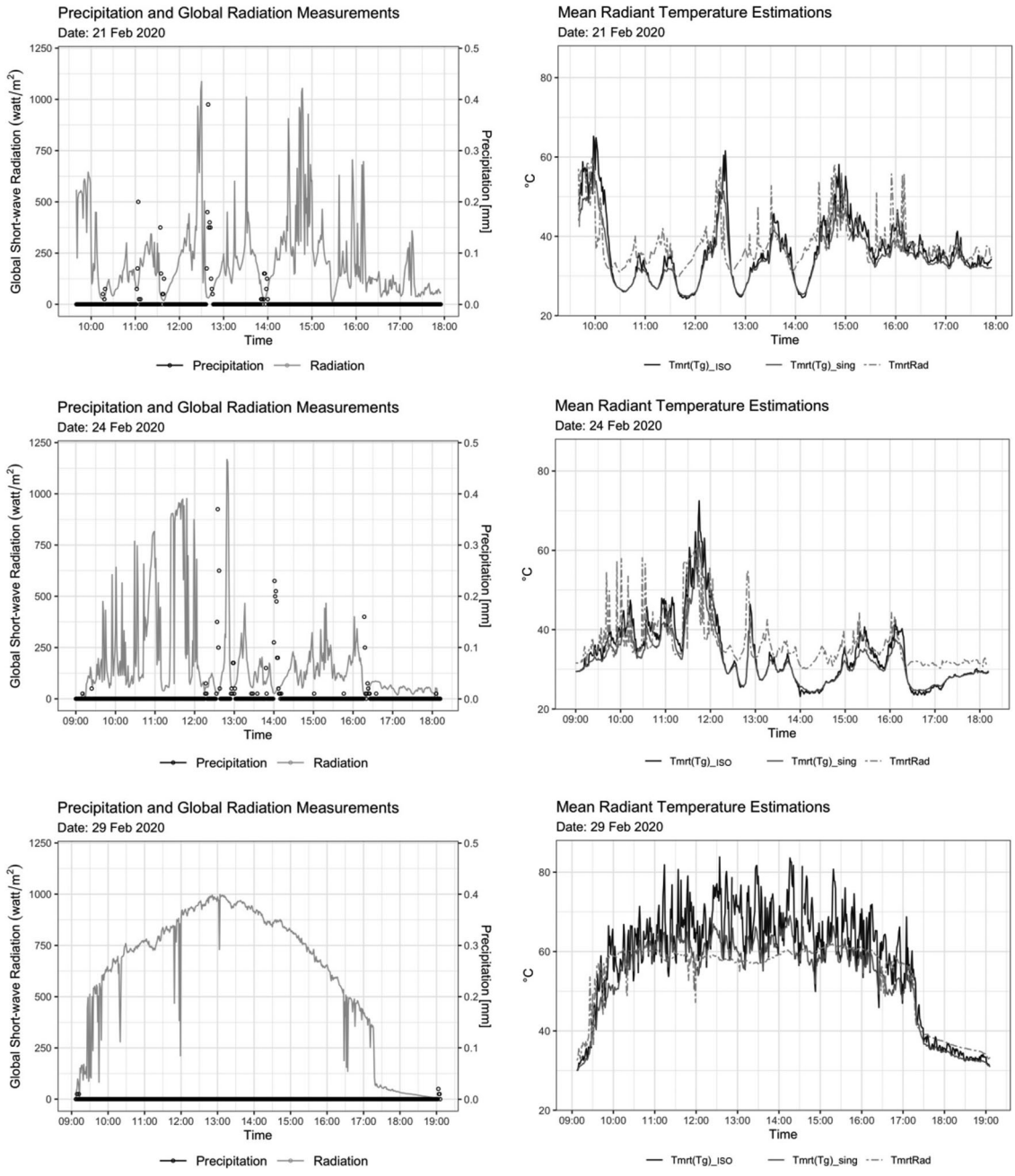

Figure 2. Left side: Global shortwave radiation and precipitation; Right side: Estimated mean radiant temperature values from T_g ($T_{mrt\ (Tg)\_ISO}$ and $T_{mrt(Tg)\_sing}$) as well as mean radiant temperature determined by integral radiation measurements and angular factors (T_{mrt_rad}) for 1 min records measured on 21st, 24th and 29th February 2020.

under the specific convective and radiative environmental conditions.

Table 2 shows the performance of T_{mrt} estimation of different mean convection coefficients derived from different averaging periods (1, 3, 5, 10, 15, 20 and 25 minute averages). Results show that the performance of $T_{mrt(Tg)\_ISO}$ and $T_{mrt(Tg)\_sing}$ improve when using mean convection coefficients of longer averaging intervals. RMSE for $T_{mrt(Tg)\_sing}$ moves from 6.8 °C for the 1-min averaged data to 4.6 °C for the 10-min averaged data. The improvement is lower when increasing from 10-min to 25-min averaged data. In this case, RMSE only reduces 1.0 °C. Similar evolution occurs for IoA. The time the globe sensors require to reach an equilibrium has been reported previously [13,14,24].

The comparison between the two $T_{mrt(Tg)}$ estimations and T_{mrt_rad} shows a better performance when using the mean convention coefficients specifically derived for Singapore ($T_{mrt(Tg)\_sing}$). The use of $T_{mrt(Tg)\_ISO}$ presents relevant periods with high overestimations, especially

Table 1. Quantitative metrics of the performance of the estimated values ($T_{mrt(Tg)\_ISO}$ and $T_{mrt(Tg)\_sing}$) with respect to mean radiant temperature determined by integral radiation measurements and angular factors (T_{mrt_rad}) for 1-min records measured on 21st, 24th and 29th February 2020.

		Dry Period		Rain/Wet Period	
		$T_{mrt(Tg)\_ISO}$	$T_{mrt(Tg)\_sing}$	$T_{mrt(Tg)\_ISO}$	$T_{mrt(Tg)\_sing}$
21/02/2020	RMSE	6.2	5.8	7.7	7.2
	$RMSE_u$	4.9	4.7	2.8	2.8
	$RMSE_s$	3.8	3.4	7.2	6.6
	MAE	4.4	4.4	6.6	6.3
	r value	0.65	0.70	−0.06	−0.04
	p value	< 2.2e-16	< 2.2e-16	0.47	0.63
	IoA	0.79	0.78	0.34	0.35
24/02/2020	RMSE	6.1	6.0	7.0	6.7
	$RMSE_u$	4.7	4.6	3.6	3.5
	$RMSE_s$	3.9	3.8	6.0	5.8
	MAE	4.6	4.7	5.9	5.7
	r value	0.74	0.75	0.36	0.40
	p value	< 2.2e-16	< 2.2e-16	1.76e-06	7.99e-08
	IoA	0.83	0.81	0.51	0.50
29/02/2020	RMSE	8.6	4.4		
	$RMSE_u$	4.5	3.5		
	$RMSE_s$	7.3	2.6		
	MAE	6.4	3.5		
	r value	0.86	0.92		
	p value	< 2.2e-16	< 2.2e-16		
	IoA	0.85	0.95		

for 1-min data. For the later, overestimations of $T_{mrt(Tg)\_ISO}$ above 10 °C occur 17.8% of the time, but it reduces to 12.8% and 8.0% for 10-min and 25-min averaged data respectively (Figure 3). In the case of $T_{mrt(Tg)\_sing}$ (Figure 4), overestimations above 10 °C occur only 0.8% of the time for the 10-minute data. However, in both cases ($T_{mrt(Tg)\_ISO}$ and $T_{mrt(Tg)\_sing}$) the percentage of time with underestimations is higher than the percentage of time with overestimation. In general, the results are better for $T_{mrt(Tg)\_sing}$. For the 10-min averaged data 45.8% of the time deviation with respect to T_{mrt_rad} is in the range of −5 °C to 0 °C, while only 31.2% of the time for $T_{mrt(Tg)\_ISO}$. As longer averaging intervals are used, the deviation of $T_{mrt(Tg)\_sing}$ in the range of −5 °C to 0 °C increases (Figure 4), while this does not happen in the case of $T_{mrt(Tg)\_ISO}$ (Figure 3). The later always shows higher deviations from T_{mrt_rad}.

Adequate averaging periods for $T_{mrt(Tg)}$ estimations depend on the size of globe thermometer but also on the fluctuation of the existing meteorological conditions [37]. Different studies have used different averaging periods (from 5 to 15 min averaging period) to estimate $T_{mrt(Tg)}$ [12–14,28,38–41].

Considering the results of the performance of $T_{mrt(Tg)\_sing}$ for different averaging periods, we select the 10-min period as a reasonable value to estimate mean radiant temperature. Climate measurements and thermal comfort analysis is meant to be representative at this temporal resolution. Furthermore the variability of cloud cover in Singapore makes it difficult to reach a final equilibrium and thus some inaccuracy has to be assumed when using the globe thermometer data. Finally, Staiger & Matzarakis [37] suggested that the black globe thermometer should not exceed averaged values of about 10 min for outdoor air velocities of ~2 (m/s), which can be considered representative of Singapore.

Table 2. Quantitative metrics of the performance of the estimated values ($T_{mrt(Tg)\_ISO}$ and $T_{mrt(Tg)\_sing}$) with respect to mean radiant temperature determined by integral radiation measurements and angular factors (T_{mrt_rad}) for different averaging periods using all the records in the campaign.

	$T_{mrt(Tg)\_ISO}$	$T_{mrt(Tg)\_sing}$
1 min average		
RMSE	8.7	6.8
RMSEu	6.5	6.1
RMSEs	5.7	2.9
MAE	6.5	5.34
r value	0.78	0.81
p value	< 2.2e-16	< 2.2e-16
IoA	0.86	0.89
3 min average		
RMSE	7.7	5.8
RMSEu	5.3	5.0
RMSEs	5.5	2.9
MAE	5.8	4.7
r value	0.84	0.86
p value	< 2.2e-16	< 2.2e-16
IoA	0.89	0.92
5 min average		
RMSE	7.2	5.3
RMSEu	4.7	4.5
RMSEs	5.4	2.8
MAE	5.4	4.3
r value	0.87	0.88
p value	< 2.2e-16	< 2.2e-16
IoA	0.90	0.93
10 min average		
RMSE	6.5	4.6
RMSEu	3.8	3.7
RMSEs	5.3	2.6
MAE	5.0	3.7
r value	0.91	0.91
p value	< 2.2e-16	< 2.2e-16
IoA	0.91	0.95
15 min average		
RMSE	6.1	4.1
RMSEu	3.3	3.3
RMSEs	5.2	2.5
MAE	4.8	3.4
r value	0.93	0.93
p value	< 2.2e-16	< 2.2e-16
IoA	0.92	0.96
20 min average		
RMSE	5.9	3.7
RMSEu	2.9	2.9
RMSEs	5.2	2.4
MAE	4.7	3.0
r value	0.95	0.95
p value	< 2.2e-16	< 2.2e-16
IoA	0.92	0.96
25 min average		
RMSE	5.8	3.6
RMSEu	2.6	2.6
RMSEs	5.2	2.4
MAE	4.6	2.9
r value	0.95	0.95
p value	< 2.2e-16	< 2.2e-16
IoA	0.92	0.96

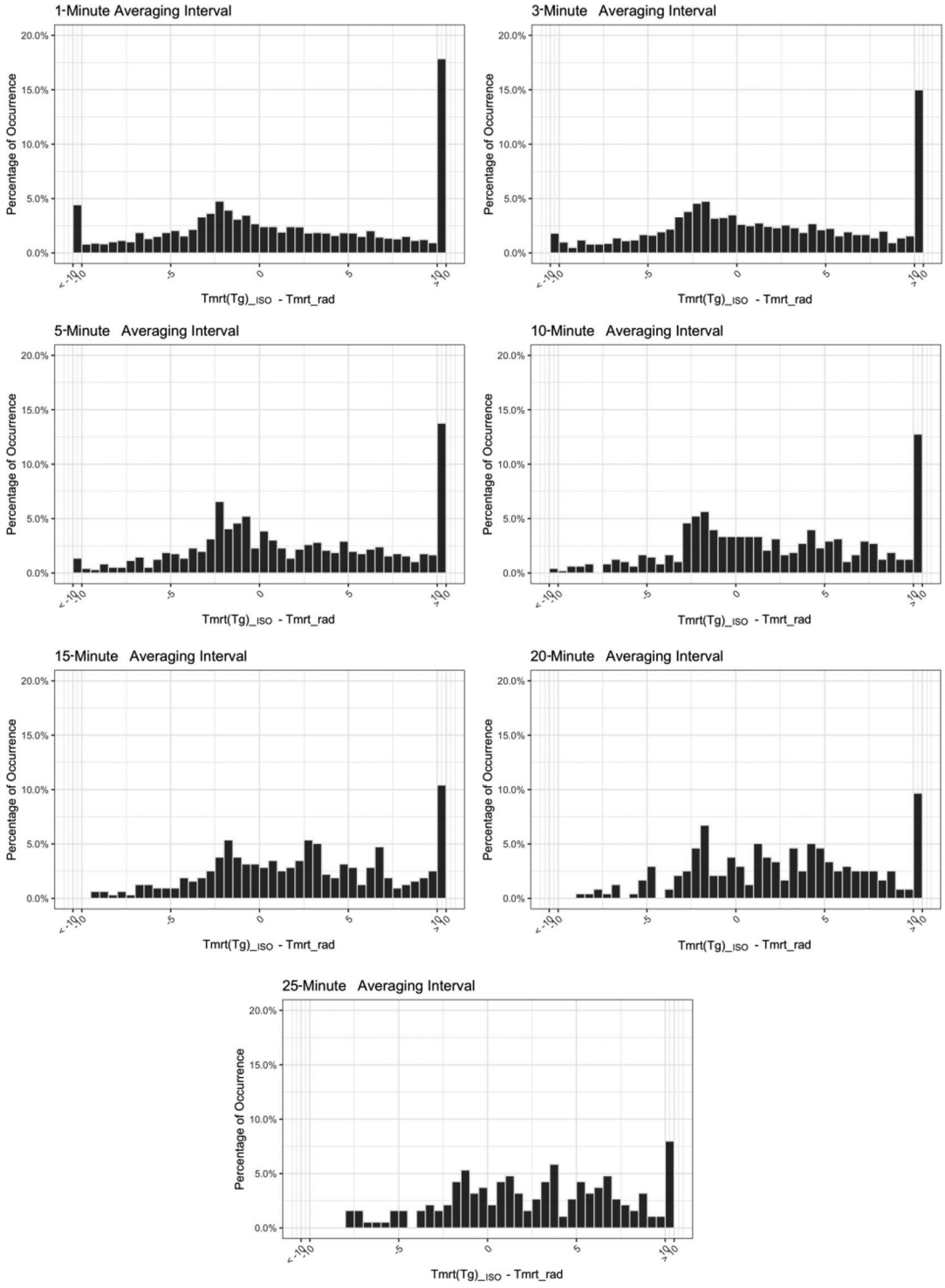

Figure 3. Frequency distribution of differences between estimated mean radiant temperature with ISO7726:1998 mean convective coefficients ($T_{mrt(Tg)\_ISO}$) and the mean radiant temperature determined by integral radiation measurements and angular factors (T_{mrt_rad}) for different averaging periods using all records measured in the campaign.

3.2.2 Suitable values for Singapore

Results in Section 3.1 have shown that in rain/wet conditions the performance of estimated $T_{mrt(Tg)\_sing}$ is different than during dry and clear skies days. However, thermal comfort in Singapore does not reach stressful levels during rain/wet conditions. Such conditions mostly occur under dry conditions. Thus, another convection coefficient for Equation (1) has been estimated by considering only dry conditions for 10 min averaging periods. The best fit shows that the

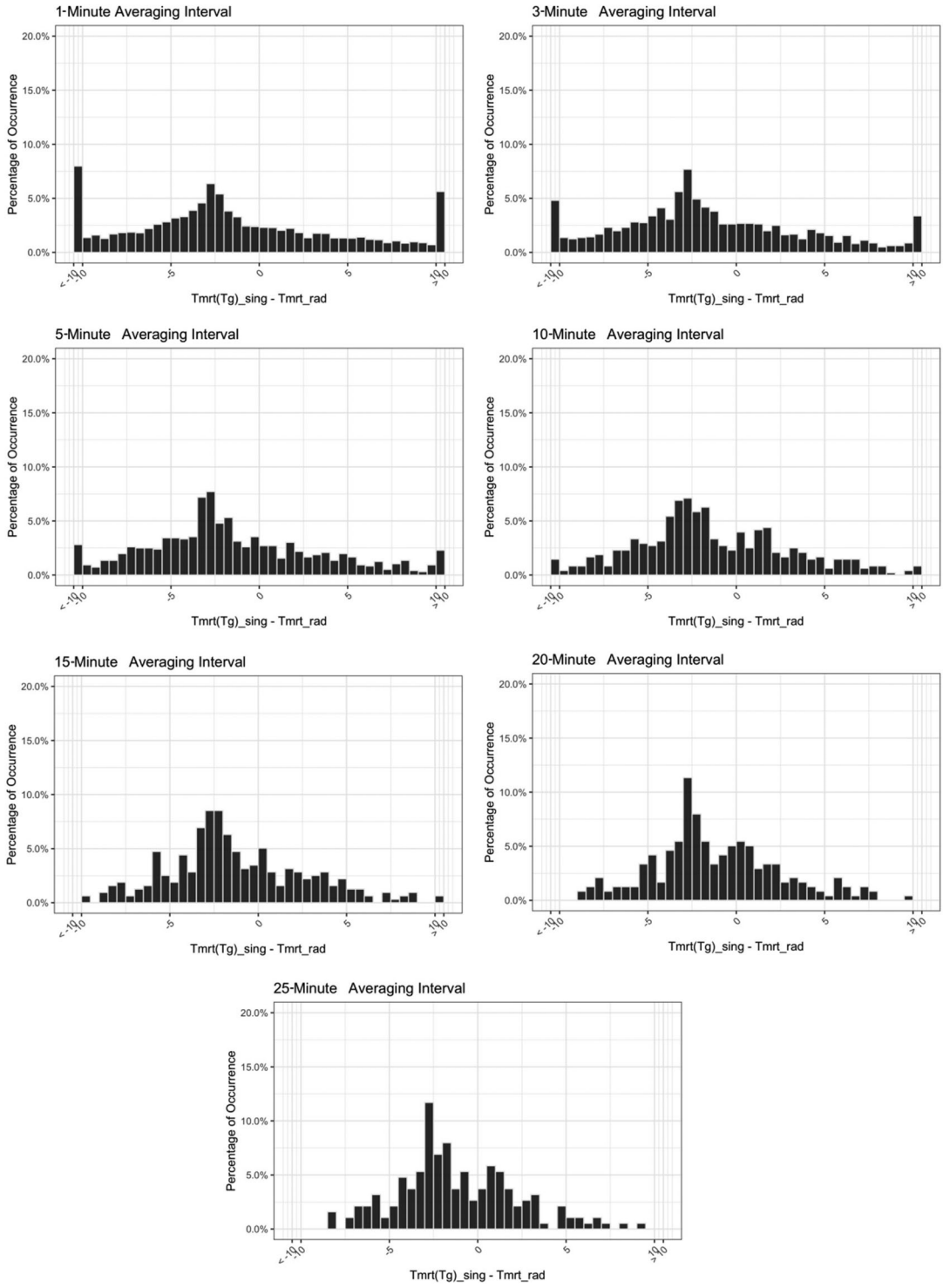

Figure 4. Frequency distribution of differences between the estimated mean radiant temperature with best fit mean convection coefficients ($T_{mrt(Tg)\_sing}$) and the mean radiant temperature determined by integral radiation measurements and angular factors (T_{mrt_rad}) for different averaging periods using all the records in the campaign.

coefficient $1.1 \cdot 10^8 \cdot V_a^{0.6}$ presented in [8] should be changed to $0.82 \cdot 10^8 \cdot V_a^{0.46}$.

The use of this new coefficient to calculate mean radiant temperature ($T_{mrt(Tg)\_sing\_nr}$) shows in three different weather conditions (21st, 24th and 29th of February) outcomes (Figure 5) similar to the ones presented in Section 3.1. During the clear sky day (29th of February) and with high incoming shortwave radiation, $T_{mrt(Tg)\_sing\_nr}$ tends to overestimate T_{mrt_rad} values. Fluctuation of $T_{mrt(Tg)\_sing\_nr}$ between 14.00 and 16.00 should

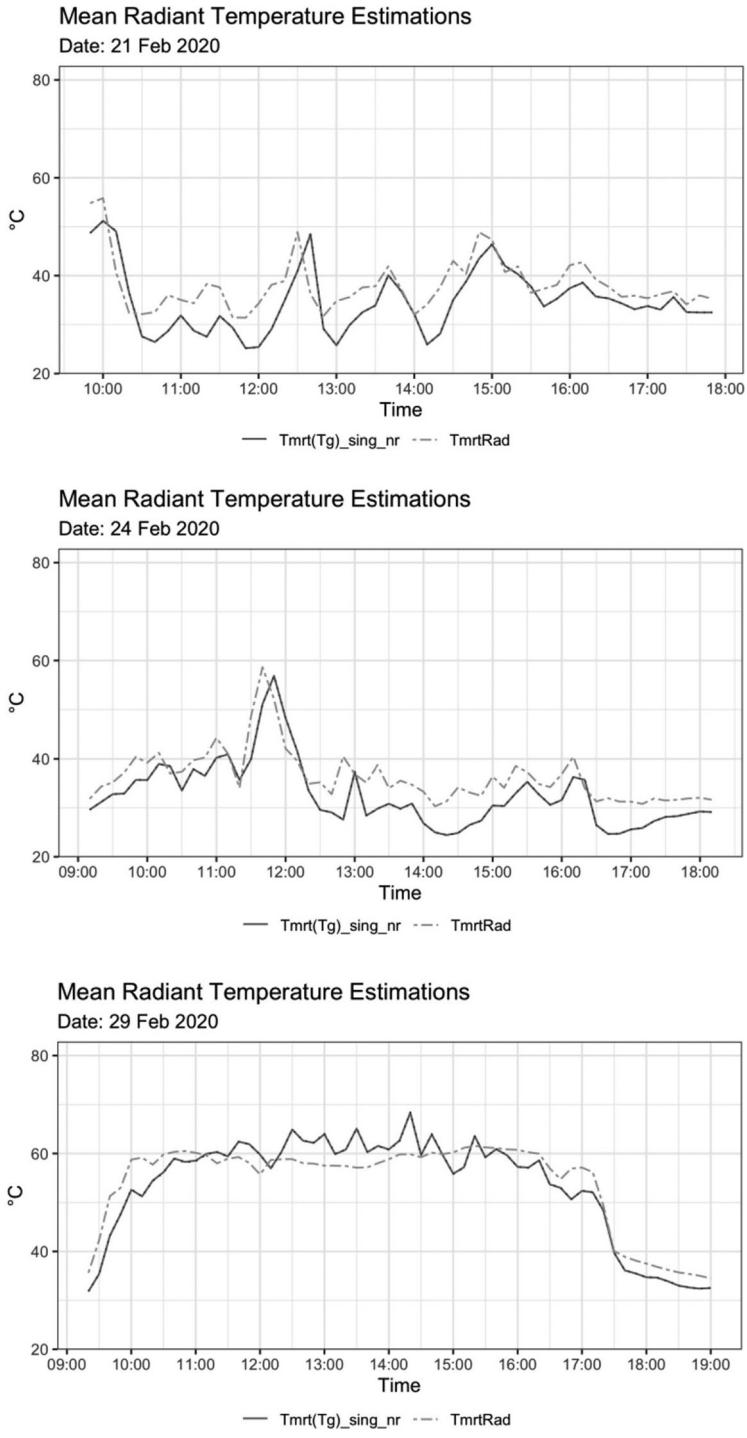

Figure 5. Estimated mean radiant temperature values using mean convective coefficients derived from dry periods ($T_{mrt(Tg)\_sing\_nr}$) as well as mean radiant temperature determined by integral radiation measurements and angular factors (T_{mrt_rad}) for 10-min records measured on 21st, 24th and 29th February 2020.

be related mostly to sharp fluctuations in V_a (1.5 ± 0.5 m s^{-1} and values ranging from 0.8–2.7 m s^{-1}). In these conditions, the performance of the globe thermometer is reduced (due to the time required to reach a thermal equilibrium due to the effects of convection and radiation) and the new mean convection coefficient is not sufficiently accurate to represent correctly T_{mrt}.

On the contrary, an underestimation occurs during the morning and evening periods. In these periods of the day with low solar elevation, the spherical form of the black globe thermometer is not able to consider correctly the approximately cylindrical shape of the human body that is reflected in T_{mrt_rad}. Similarly, under shaded conditions (e.g. 29th February after 17.15) and overcast

Table 3. Quantitative metrics of the performance of the estimated mean radiant temperature values using mean convective coefficients derived from dry periods ($T_{mrt\ (Tg)\_sing\_nr}$) with respect to mean radiant temperature determined by integral radiation measurements and angular factors (T_{mrt_rad}) for 10-min records measured on 21st, 24th and 29th February 2020.

	21/02/2020	24/02/2020	29/02/2020
RMSE	5.4	5.0	3.9
RMSEu	3.5	2.7	3.0
RMSEs	4.2	4.3	2.4
MAE	4.5	4.4	3.3
r value	0.77	0.86	0.94
p value	1.30E-10	< 2.2e-16	< 2.2e-16
IoA	0.80	0.84	0.96

conditions (e.g. 21st February after 15:30) $T_{mrt(Tg)\_sing\_nr}$ also tends to underestimate T_{mrt_rad}. However, this underestimation is especially relevant during rain/wet periods while the sensors remain wet (e.g. 21st and 24th February after 14:00) as commented in Section 3.1.

The performance of $T_{mrt(Tg)\_sing\_nr}$ for different type of days is shown in Table 3. Quantitative metrics show a much better performance during the clear skies days (29th February), an outcome of using the convection coefficient estimated only in dry periods ($0.82{\cdot}10^8{\cdot}V_a^{0.46}$). During this day, RMSE is 3.9 °C with $RMSE_u$ higher than $RMSE_s$. This represents a relevant improvement with respect to the performance of ISO7726 coefficients (RMSE = 7.4 °C). For the overcast and rainy days RMSE raises to 5.4 °C and 5.0 °C on the 21st and 24th February respectively with relevant systematic underestimation ($RMSE_s > RMSE_u$). Other metrics as MAE, r value and IoA also indicate good results and suitability of the mean convection coefficient ($0.82{\cdot}10^8{\cdot}V_a^{0.46}$) derived for Singapore. The level of accuracy is similar to other attempts to calibrate globe sensors for T_{mrt} estimations [13,28].

4. Conclusions

One of the more complex variables required to evaluate outdoor thermal comfort is T_{mrt}. Different methods to measure T_{mrt} are available, although they require different resources and costs can differ significantly. In this paper we adapt the formula that translates globe temperature measurements into T_{mrt} [8] by providing a new and more accurate mean convection coefficient for the Singapore context. This coefficient is derived by means of T_{mrt} calculated from integral radiation measurements and meteorological variables T_g, T_a and V_a.

Results show a relevant improvement in the estimation of $T_{mrt(Tg)}$ when using a calibrated mean convection coefficient in comparison with the default coefficient presented in [8]. This is especially noticed during clear skies and high incoming solar radiation. In these weather conditions estimations of $T_{mrt(Tg)}$ always tend to overestimate accurate values derived from the integral radiation measurements. On the contrary, during rain/wet conditions $T_{mrt(Tg)}$ is underestimated. In this case, both mean convection coefficients (default and calibrated) show similar results. Finally, under shadow conditions and low incoming solar radiation (dry overcast) conditions, $T_{mrt(Tg)}$ estimations tend to present less deviation. On the whole, results have shown that the same mean convection coefficient performs differently in diverse weather conditions.

Quick changes in incoming solar radiation and wind speed are not considered correctly by the globe thermometer, causing relevant deviation in $T_{mrt(Tg)}$ estimations. Smoothing this environmental changes by increasing the averaging period can improve the performance. When using moving from 1-min to 10-min averaged values, RMSE is reduced from 6.8 °C to 4.6 °C.

Finally, we apply a mean convection coefficient ($0.82{\cdot}10^8{\cdot}V_a^{0.46}$) that best suits the uncomfortable thermal conditions of Singapore (i.e. dry periods). In the case of a clear skies day, RMSE can be reduced to 3.9 °C.

However, results have shown that under transient climatic conditions, the calibration of mean convection coefficient can provide inaccurate T_{mrt} values.

This work provides the possibility to improve the estimation of T_{mrt} in outdoor settings in a hot, humid, low wind speed and cloudy tropical region like Singapore by using a 150 mm black globe thermometer. The approach is simple and requires significantly less costs than radiation measurements. The 10-min mean convection coefficient presented is valuable for thermal comfort assessment.

Acknowledgments

We would like to thank Prof. Wong Nyuk Hien (National University of Singapore) for sharing the radiometers used for this work, and also Dr. Cuauhtemoc Anda (Future Cities Lab, SEC) for the help provided.

Disclosure statement

No potential conflict of interest was reported by the author(s).

Funding

This research is supported by the Singapore National Research Foundation under its Campus for Research Excellence and Technological Enterprise (CREATE) programme and its "Cooling Singapore" collaborative project (Grant number:

NRF2019VSG-UCD-001) led by the Singapore-ETH Centre (SEC), with Singapore MIT Alliance for Research and Technology (SMART), TUMCREATE (established by the Technical University of Munich), the National University of Singapore (NUS) and the Singapore Management University (SMU).

Data availability statement

The data that support the findings of this study are available on request from the authors J. A. Acero and A. Dissegna. Restrictions apply to the availability of these data, which were used for this study. Data are available from authors J. A. Acero and A. Dissegna with the permission of Singapore National Research Foundation (NRF).

ORCID

Juan A. Acero http://orcid.org/0000-0001-6214-0605

References

[1] VDI-3787. (2008). *Environmental Meteorology Methods for the Human Biometeorological Evaluation of Climate and Air Quality for Urban and Regional Planning at Regional Level. Part 1 Climate. Verlag des Vereins Deutscher Ingenieure*. Düsseldorf, Germany.

[2] da Silva TGF, Santos GCL, Duarte AMC, et al. Black globe temperature from meteorological data and a bioclimatic analysis of the Brazilian northeast for saanen goats. J Therm Biol. 2019;85:102408-17.

[3] Acero JA, Herranz-Pascual K. A comparison of thermal comfort conditions in four urban spaces by means of measurements and modelling techniques. Build Environ. 2015;93:245–257. doi:10.1016/j.buildenv.2015.06.028.

[4] Cohen P, Potchter O, Matzarakis A. Daily and seasonal climatic conditions of Green urban open spaces in the Mediterranean climate and their impact on human comfort. Build Environ. 2012;51:285–295. doi:10.1016/j.buildenv.2011.11.020.

[5] Kántor N, Unger J. The most problematic variable in the course of human-biometeorological comfort assessment – the mean radiant temperature. Central European Journal of Geosciences. 2011;3(1):90–100..

[6] Lin TP, Matzarakis A, Hwang RL. Shading effect on long-term outdoor thermal comfort. Build Environ. 2010;45(1):213–221. doi:10.1016/j.buildenv.2009.06.002.

[7] Mayer H, Holst J, Dostal P, et al. Human thermal comfort in summer within an urban street canyon in Central Europe. Meteorol Z. 2008;17(3):241–250. doi:10.1127/0941-2948/2008/0285.

[8] ISO7726. Ergonomics of the thermal environment – Instruments for measuring physical quantities. Geneva: International Standarization Organization; 1998.

[9] Du J, Sun C, Xiao Q, et al. Field assessment of winter outdoor 3-D radiant environment and its impact on thermal comfort in a severely cold region. Sci Total Environ. 2020;709:136175-98.

[10] Gál CV, Kántor N. Modeling mean radiant temperature in outdoor spaces, A comparative numerical simulation and validation study. Urban Climate. 2020;32(April 2019):100571-86. doi:10.1016/j.uclim.2019.100571.

[11] Acero JA, Arrizabalaga J. Evaluating the performance of ENVI-met model in diurnal cycles for different meteorological conditions. Theor Appl Climatol. 2018;131(1–2):455–469. doi:10.1007/s00704-016-1971-y.

[12] Kántor N, Kovács A, Lin T-P. Looking for simple correction functions between the mean radiant temperature from the "standard black globe" and the "six-directional" techniques in Taiwan. Theor Appl Climatol. 2015;121(1–2):99–111. doi:10.1007/s00704-014-1211-2.

[13] Thorsson S, Lindberg F, Eliasson I, et al. Different methods for estimating the mean radiant temperature in an outdoor urban setting. Int J Climatol. 2007;27:1983–1993. doi:10.1002/joc.1537.

[14] Chen YC, Lin TP, Matzarakis A. Comparison of mean radiant temperature from field experiment and modelling: a case study in freiburg, Germany. Theor Appl Climatol. 2014;118(3):535–551. doi:10.1007/s00704-013-1081-z.

[15] de Dear R. Ping-Pong globe thermometers for mean radiant temperatures. H and V Engineer. 1987;60(681):10–11.

[16] Kuehn LA, Stubbs RA, Weaver RS. Theory of the globe thermometer. J Appl Physiol Respir Environ Exerc Physiol. 1970;29(5):750–757. doi.10.1152/jappl.1970.29.5.750.

[17] Nikolopoulou M, Baker N, Steemers K. Improvements to the globe thermometer for outdoor Use. Archit Sci Rev. 1999;42(1):27–34 doi.10.1080/00038628.1999.9696845.

[18] Guo H, Teitelbaum E, Houchois N, et al. Revisiting the use of globe thermometers to estimate radiant temperature in studies of heating and ventilation. Energy Build. 2018;180:83–94.

[19] d'Ambrosio Alfano FR, Dell'isola M, Ficco G, et al. On the measurement of the mean radiant temperature by means of globes: An experimental investigation under black enclosure conditions. Build Environ. 2021;193:107655–66.

[20] d'Ambrosio Alfano FR, Ficco G, Frattolillo A, et al. Mean radiant temperature measurements through small black globes under forced convection conditions. Atmosphere (Basel). 2021;12(5):621–633.

[21] Matzarakis A, Rutz F, Mayer H. Modelling radiation fluxes in simple and complex environments: basics of the RayMan model. Int J Biometeorol. 2010;54(2):131–139 doi.10.1007/s00484-009-0261-0.

[22] Bruse M, Fleer H. Simulating surface-plant-air interactions inside urban environments with a three dimensional numerical model. Environmental Modelling and Software. 1998;13:373–384. doi:10.1016/S1364-8152(98)00042-5.

[23] Lindberg F, Holmer B, Thorsson S. SOLWEIG 1.0 - Modelling spatial variations of 3D radiant fluxes and mean radiant temperature in complex urban settings. Int J Biometeorol. 2008;52(7):697–713. doi:10.1007/s00484-008-0162-7.

[24] McIntyre D. Indoor climate. London: Architectural Publication Series; 1980.

[25] Hey EN. Small globe thermometers. J Phys E Sci Instrum. 1968;1(9):424–431.

[26] Teitelbaum E, Chen KW, Meggers F, et al. Globe thermometer free convection error potentials. Sci Rep. 2020;10(1):1–13. doi:10.1038/s41598-020-59441-1.

[27] Manavvi S, Rajasekar E. Estimating outdoor mean radiant temperature in a humid subtropical climate. Build Environ. 2020;171:106658. doi:10.1016/j.buildenv.2020.106658.
[28] Tan CL, Wong NH, Jusuf SK. Outdoor mean radiant temperature estimation in the tropical urban environment. Build Environ. 2013;64:118–129. doi:10.1016/j.buildenv.2013.03.012.
[29] Roth M, Chow WTL. A historical review and assessment of urban heat island research in Singapore. Singap J Trop Geogr. 2012;33(3):381–397. doi:10.1111/sjtg.12003.
[30] Chow WTL, Roth M. Temporal dynamics of the urban heat island o Singapore. Int J Climatol. 2006;26(26):2243–2260. doi:10.1002/joc.1364.
[31] Beck F, Bárdossy A, Seidel J, et al. Statistical analysis of sub-daily precipitation extremes in Singapore. Journal of Hydrology: Regional Studies. 2015;3:337–358. doi:10.1016/j.ejrh.2015.02.001.
[32] Mandapaka PV, Qin X. Analysis and characterization of probability distribution and small-scale spatial variability of rainfall in Singapore using a dense gauge network. Journal of Applied Meteorology and Climatology. 2013;52(12):2781–2796. doi:10.1175/JAMC-D-13-0115.1.
[33] Hoppe P. Ein neues Verfahren zur Bestimmung der mittleren Strahlungstemperatur in Freien. Wetter und Leben. 1992;44:147–151.
[34] Holmer B, Lindberg F, Rayner D, et al. (2015). *How to transform the standing man from a box to a cylinder – A modified methodology to calculate mean radiant temperature in field studies and models*. In *9th International Conference on Urban Climate (ICUC9)*. Toulouse (France).
[35] Dissegna MA, Yin T, Wu H, et al. Modeling mean radiant temperature distribution in urban landscapes using DART. Remote Sens (Basel). 2021;13(8):1443–1455. doi.10.3390/rs13081443.
[36] Willmott C. Some comments on the evaluation of model performance. B Am Meteorol Soc. 1982;63:1309–1369.
[37] Staiger H, Matzarakis A. Accuracy of mean radiant temperature derived from active and passive radiometry. Atmosphere (Basel). 2020;11(8):805–817. doi.10.3390/ATMOS11080805.
[38] Kántor N, Gál CV, Gulyás Á, et al. The impact of façade orientation and woody vegetation on summertime heat stress patterns in a Central European square: comparison of radiation measurements and simulations. Advances in Meteorology. 2018;2018:1–15. doi.10.1155/2018/2650642.
[39] Krüger EL, Minella FO, Matzarakis A. Comparison of different methods of estimating the mean radiant temperature in outdoor thermal comfort studies. Int J Biometeorol. 2014;58(8):1727–1737. doi: 10.1007/s00484-013-0777-1.
[40] Marino C, Nucara A, Pietrafesa M, et al. (2018). Outdoor Mean Radiant Temperature Estimation: Is the Black-Globe Thermometer Method a Feasible Course of Action? In *Proceedings - 2018 IEEE International Conference on Environment and Electrical Engineering and 2018 IEEE Industrial and Commercial Power Systems Europe, EEEIC/I and CPS Europe* 2018. doi:10.1109/EEEIC.2018.8493714.
[41] Ndetto EL, Matzarakis A. Assessment of human thermal perception in the hot-humid climate of Dar es Salaam, Tanzania. Int J Biometeorol. 2017;61(1):69–85. doi: 10.1007/s00484-016-1192-1.